CREEP ANALYSIS OF A PROCESS TUBE

T.H. LIN,
University of California, Los Angeles, California

D.R. ANDERSON,
Atomics International,
North American Rockwell, Canoga Park, California,

W.F. ANDERSON,
Liquid Metal Engineering Center,
Canoga Park, California, U.S.A.

ABSTRACT

A process tube of a nuclear reactor cooled by liquid sodium, subject to a variation of temperature of 750°F to 1200°F and a variation of internal pressure along the length is analyzed. This tube made of 304 stainless steel, is designed for a life of 30 years..

Based on creep data in terms of tensile stress vs temperature at creep ratios of 0.0001% and 0.00001% per hour, the stress vs. temperature for lower creep rates are extrapolated by hyperbole sine law. This uniaxial stress-strain-time relationship is generalized for multiaxial stress. The creep strain components are assumed to be propertional to the corresponding deviated stress components and a function of the second deviate stress invariant.

The change of stress caused by the incremental creep strain is obtained by the analogy of creep strain gradient and the applied body force similar to Duhamel' s analogy for thermal strain. The differential equation for the bending of the tube is written in finite difference form and solved with the aid of an IBM computer. The deflected curves and the maximum longitudinal stress of the process tube at different stages of its life are calculated and shown.

1. INTRODUCTION

This analysis is for the design of a process tube in a nuclear reactor cooled by liquid sodium. The upper end of the process tube is brazed to the top plate of the calandria shell and the lower end slides vertically over a liner attached to the bottom plate of the shell. This allows the tube to expand freely in the longitudinal direction. Due to the differential thermal expansion of the top and bottom of the calandria shell, the top end of the tube moves outward relative to the lower end during operation. This relative displacement has been estimated to be about 0.35". A sketch of the process tube is shown in Fig. 1. The top end deflects with the top plate of the shell and is assumed to have an angle β with the vertical during operation. $\beta = 0.01$ radian is assumed for this analysis. Due to this rotation β, the lower end of the tube moves inward and hits the guide

tube, which exerts a horizontal force Y_o at the lower end as shown.

This tube is subject to a net internal pressure varying linearly from 22 p. s. i. at the bottom to 15 p. s. i. at the top. The fuel elements are attached to the lower end of the tube and have a submerged weight of 263 pounds. These fuel elements are very flexible in bending and shear. They run inside the process tube and are supported by spacers at equal spacings along the length of the tube. A bellow is attached to the lower end. The internal pressure in the bellow tends to push the lower end upward and exerts a compression on the tube. To reduce the compression, the lower end carries graphite blocks of 330 pounds.

The lower portion of the tube containing the active fuel elements has a wall thickness of 0. 025". In the upper portion, the temperature is high and there is no active fuel element, so the increase of wall thickness there has no harmful effect on the efficiency of the operation. In this portion, a wall thickness of 1/8" is used to provide higher creep flexural rigidity.

2. METHOD OF ANALYSIS

Effect of Internal Pressure and Fuel Weight: When a tube under internal pressure bends, the convex side lengthens while the concave side shortens. (Fig. 2). The lateral area of the convex side exceeds that of the concave side. This excess of lateral area times the net internal pressure induces a lateral load, which in turn, causes the pulse to bend further. Hence, a tube under internal pressure may buckle just like a column under a compressive load. This phenomenon is known and applied to the present analysis. Referring to Fig. 2, when an elemental length dx of the tube is bent with a radius of curvature R, the original length dx at a distance η from the neutral axis becomes

$$dx' = dx \left(1 + \frac{\eta}{R}\right) \tag{1}$$

with $\eta = r_i \cos \theta$, where r_i is the inner radius of the tube

$$dx' - dx = \frac{r_i \cos \theta}{R} dx \tag{2}$$

This gives an increase of a projected lateral area per unit length of

$$\int_o^{2\pi} \frac{r_i \cos \theta}{R} r_i \cos \theta \, d\theta = \frac{\pi r_i^2}{R}$$

and an increase of lateral load q_1 per unit length of

$$\frac{\pi p r_i^2}{R}$$

With w denoting the lateral deflection of the tube

$$\frac{1}{R} \cong - \frac{d^2w}{dx^2} \tag{3}$$

$$q_1 = - \pi p r_1^2 \frac{d^2w}{dx^2} \tag{4}$$

The fuel elements are flexible in shear and in bending and are assumed to have no resistance to tube deflection. The resultant compressive force due to fuel elements weight is along the deflected curve of the tube. Referring to Fig. 3, with $\frac{d^2w}{dx^2}$ representing the curvature, $\overline{W}$ the weight of the fuel elements above the particular section x, the horizontal components of the compressive axial forces at the two ends of the element dx have a net horizontal force of $- \overline{W} \frac{d^2w}{dx^2}$ dx. This gives a lateral load of $q_2 = - \overline{W} \frac{d^2w}{dx^2}$ per unit length. The fuel elements weight has the same effort in causing additional lateral load as the internal pressure. Due to the presence of fuel weight and internal pressure, the process tube behaves like a column subject to creep.

Creep buckling of simple columns has been studied by many investigators. Shanley [1] 1950 proposed the use of isochronous tangent modulus for creep buckling of columns. It is well known that this procedure gives a low estimate of column life [2]. For columns of uniform section under uniform temperature, methods for creep analysis have been given by Higgins [3], Libove [4], Hoff [5] and Lin [6,7]. But creep analysis for columns with varying internal pressure and varying temperature along the column length, seems to be scarce. The following method is developed for this analysis.

$$q = q_1 + q_2 = - \left(\pi p r_i^2 + \overline{W} \right) \frac{d^2w}{dx^2} \tag{5}$$

p and $\overline{W}$ both mainly vary linearly with x. $\left(\pi r_i^2 p + \overline{W} \right)$ is expressed as $q_o + bx$. Let P_1 denote the compressive load exerted by the pressure in the bellow, A_o the internal cross-section area of the tube, G the graphite weight. Referring to Fig. 1, the bending moment at section x is

$$M = x Y_o - P_1 \left[x \left(\frac{dw}{dx} \right)_{x=0} - w \right] - \int_o^x \int_o^x q \, dxdx - Gw = - EI \frac{d^2w}{dx^2} \tag{6}$$

where E is the Young's modulus and I the rectangular moment of inertia of the tube. Substituting the expression $q_o + bx$ for q in the integral and integrating, we have

$$\int_o^x \int_o^x q \, dxdx = A_o q_o \left[W - x \left(\frac{dw}{dx} \right)_{x=0} \right] + A_o b \left[xw - 2 \int_o^x w \, dx \right] \tag{7}$$

Substituting this into Eq. (6) yields

$$M = x\,Y_o - P_1\left[x\left(\frac{dw}{dx}\right)_{x=0} - w\right] + A_o\,q_o\left[w - x\left(\frac{dw}{dx}\right)_{x=0}\right]$$

$$+ A_o\,b\left[x\,w - 2\int_o^x w\,dx\right] - G\,w = -EI\,\frac{d^2w}{dx^2} \qquad (8)$$

This is the differential equation of equilibrium of the tube with no creep.

Creep Strain Calculations: The process tube is of 304 stainless steel. Creep data of this steel taken from ASTM Boiler Code are referred to as Data I. Another set of creep data obtained by the materials laboratory of Atomic International is referred to as Data II. These two sets of data give stress vs. temperature corresponding to creep rates of 0.0001% and 0.00001% per hour. There is a considerable amount of scatter in both sets. The lower bound curves of these data are shown in Figs. 4 and 5. The lower bound curves of Data II were used for the present analysis. Data I are shown for comparison. The stress in the process tube for the major portion of the tube life is much smaller than that corresponding to a creep rate of 0.00001% per hour. Hence, these creep data must be extrapolated to the low stress level. McVetty [8] has shown that power law extrapolation may give non-conservative creep rates in low stress levels, so here hyperbolic sine law proposed by Nadai [9] is used for extrapolation. In the present calculations, power law is used between .0001% and .00001% per hour creep rates and hyperbolic sine law is used to extrapolate the stress for creep rates less than .00001% per hour. This extrapolation laws are so chosen in order to be conservative [10].

Axial, bending and hoop stresses exist in the process tube, so a method to calculate the rate of complex creep strain is required. Considerable amount of test data or creep under complex stress system has been carried out by Johnson [11] and Henderson. The principal axes of stress and creep strain rate are taken to coincide, up to moderate degree of creep strain. The volumetric change due to creep strain is negligible and the hydrostatic stress is taken to have no effect on creep. These assumptions have satisfactory experimental support in the calculation of the multiaxial creep strain rate, the plastic yield criterion of Mises-Hencky [12] (i.e., the second invariant of the deviated stress) is used. The rates of creep strain components are proportional to the corresponding deviated stress components. Referring to a set of rectangular axes x_1, x_2 and x_3, the rate of creep strain component ϵ_{ij} may be expressed as

$$\epsilon_{ij} = F(\bar{J}_2)\,S_{ij} \qquad (9)$$

where S_{ij} is the deviated stress component. F is a function and $\bar{J}_2$ is the second deviated-stress invariant. Soderberg [13] has presented the similar relation in the following form

$$\dot{\epsilon}_1 = \frac{\dot{\epsilon}^*}{\sigma^*}\left[\sigma_1 - \frac{1}{2}(\sigma_2 + \sigma_3)\right]$$

$$\dot{\epsilon}_2 = \frac{\dot{\epsilon}^*}{\sigma^*}\left[\sigma_2 - \frac{1}{2}(\sigma_1 + \sigma_3)\right] \qquad (10)$$

$$\dot{\epsilon}_3 = \frac{\dot{\epsilon}^*}{\sigma}\left[\sigma_3 - \frac{1}{2}(\sigma_1 + \sigma_2)\right]$$

where σ_1, σ_2 and σ_3 are principal stresses; and ϵ_1, ϵ_2 and ϵ_3 are principal creep strain rates and

$$\sigma^* = \frac{1}{\sqrt{2}}\left[(\sigma_1 - \sigma_2)^2 + (\sigma_2 - \sigma_3)^2 + (\sigma_3 - \sigma_1)^2\right]^{1/2}$$

$$\dot{\epsilon}^* = \frac{\sqrt{2}}{3}\left[(\dot{\epsilon}_1 - \dot{\epsilon}_2)^2 + (\dot{\epsilon}_2 - \dot{\epsilon}_3)^2 + (\dot{\epsilon}_3 - \dot{\epsilon}_1)^2\right]^{1/2} \qquad (11)$$

In tensile test, σ^* and ϵ^* reduce to tensile stress and tensile strain, respectively. In the present case the longitudinal stress σ_x corresponds to σ_1 and the hoop stress σ_θ corresponds to σ_2 and $\sigma_3 = 0$. Consider a particular point in the process tube. The stress, either σ_x or σ_θ, vs. time is generally a smooth curve. For one numerical calculation, this smooth stress-time curve is often approximated by horizontal and vertical segments [6, 7] as shown in Fig. 6. Within each Δt, the stresses σ_x and σ_θ are assumed constant. Following each constant stress period Δt, there is an instantaneous change of stress $\Delta\sigma$. The incremental creep strains $\Delta\epsilon_x$ and $\Delta\epsilon_\theta$ in the period Δt are obtained from the steady creep rate vs. stress relation at the particular temperature. The error introduced through keeping the stresses constant in Δt decreases to zero as Δt approaches zero.

The axial stress

$$\sigma_x = -\left(\frac{P}{A} + \frac{M\eta}{I}\right) \qquad (12)$$

and the hoop stress

$$\sigma_\theta = \frac{(p_i - p_o)r}{t} \qquad (13)$$

where P is the compressive load, A the cross-section area, I the rectangular moment of inertia, p_i and p_o are the internal and external pressures, respectively. The radial stress and the longitudinal shear stress are small and are neglected. The effective stress σ^* and the effective creep strain rate $\dot{\epsilon}^*$ reduce to

$$\sigma^* = \frac{1}{\sqrt{2}}\left[(\sigma_x - \sigma_\theta)^2 + \sigma_x^2 + \sigma_\theta^2\right]^{1/2} \qquad (14)$$

$$\dot{\epsilon}^* = \frac{\sqrt{2}}{3}\left[(\dot{\epsilon}_x - \dot{\epsilon}_\theta)^2 + (\dot{\epsilon}_\theta - \dot{\epsilon}_r)^2 + (\dot{\epsilon}_r - \dot{\epsilon}_x)^2\right]^{1/2} \qquad (15)$$

Equation (10) reduces to

$$\dot{\epsilon}_x = \frac{\dot{\epsilon}^*}{\sigma^*}\left(\sigma_x - \frac{1}{2}\sigma_\theta\right) \tag{16}$$

$$\dot{\epsilon}_\theta = \frac{\dot{\epsilon}^*}{\sigma^*}\left(\sigma_\theta - \frac{1}{2}\sigma_x\right) \tag{17}$$

In a time increment Δt, the incremental creep strain components are

$$\Delta\epsilon_x = \dot{\epsilon}_x \Delta t \;;\; \Delta\epsilon_\theta = \dot{\epsilon}_\theta \Delta t \tag{18}$$

The elastic strain components are related to stresses as

$$e'_x = \frac{1}{E}\left(\sigma_x - \nu\sigma_\theta\right) \;;\; \epsilon'_\theta = \frac{1}{E}\left(\sigma_\theta - \nu\sigma_x\right) \tag{19}$$

where ν is Poisson's ratio and E is Young's modulus. Taking the elastic strain as the difference between the total strain e_x, e_θ and the creep strain, from Eq. (19)

$$\Delta\sigma_x = \frac{E}{1-\nu^2}\left[\Delta e_x + \nu\Delta e_\theta - \Delta\epsilon_x - \nu\Delta\epsilon_\theta\right] \tag{20}$$

$$\Delta\sigma_\theta = \frac{E}{1-\nu^2}\left[\Delta e_\theta + \nu\Delta e_x - \Delta\epsilon_\theta - \nu\Delta\epsilon_x\right] \tag{21}$$

Since hoop tension remains constant, it is assumed that $\Delta\sigma_\theta = 0$ at every point. This gives

$$\Delta\sigma_x = E\left(\Delta e_x - \Delta\epsilon_x\right) \tag{22}$$

The total axial load P remains constant

$$\Delta P = \int \Delta\sigma_x \, dA = E\int\left(\Delta e_x - \Delta\epsilon_x\right) dA = 0 \tag{23}$$

From Berhoulli and Euler's assumption that plane in the column before deformation remains plane during deformation

$$\Delta e_x = \Delta e_{x_o} + \eta\frac{d^2\Delta w}{dx^2} \tag{24}$$

where the subscription "0" denotes the centroidal axis, the signs of η and w are shown in Figs. 1 and 2, and ϵ_x is positive for tension. Substituting Eq. (24) into Eq. (23), we have

$$\Delta e_{x_o} = \frac{1}{A}\int \Delta\epsilon_x \, dA = \Delta\bar{\epsilon}_x \;,$$

which is the average longitudinal creep strain over the cross-section.

$$\Delta\sigma_x = E\left[\Delta\bar{\epsilon}_x + \eta\frac{d^2\Delta w}{dx^2} - \Delta\epsilon_x\right] \tag{25}$$

$$\Delta M = -\int \Delta\sigma_x \, \eta \, dA$$

$$= -\int \left[\Delta\bar{\epsilon}_x + \eta \frac{d^2\Delta w}{dx^2} - \Delta\epsilon_x\right] \eta \, dA$$

$$\Delta M = -EI \frac{d^2\Delta w}{dx^2} + E\int \Delta\epsilon_x \, \eta \, dA \qquad (26)$$

Hence, the resisting moment of the section is relaxed by the amount $E\int \Delta\epsilon_x \, \eta \, dA$. Writing Eq. (8) in incremental form and substituting Eq. (26) for ΔM, we have

$$\Delta M = x\Delta Y_o - P_1\left[\left(\frac{d\Delta w}{dx}\right)_{x=0} x - \Delta w\right] + A_o q_o\left[\Delta w - x\left(\frac{d\Delta w}{dx}\right)_{x=0}\right]$$

$$+ b A_o\left[x\Delta w - 2\int_o^x \Delta w \, dx\right] = -EI \frac{d^2\Delta w}{dx^2} + E\int \Delta\epsilon_x \, \eta \, dA \qquad (27)$$

For an incremental time interval Δe, the stresses σ_x, σ_θ are known and assumed to be constant in this time interval. The tube is divided into a number of segments. $\Delta\epsilon_x$ and $\Delta\epsilon_\theta$ are computed at different grid points on different sections of the tube. Then the incremental relaxed moments expressed by the integral in Eq. (27) at different sections are evaluated. Then Eq. (28) is written in finite difference form and applied to different sections of the tube. The values of the incremental deflections Δw' s of different sections are obtained from the solution of a set of simultaneous equations. These incremental deflections at different points are added to deflections at the beginning of Δt to obtain the deflections at the end of Δt, which is equal to those at the beginning of the subsequent time interval. This process is repeated for each time increment for the designed life of the tube. The bending moment at each section is then

$$M = -EI \frac{d^2w}{dx^2} + E\int \epsilon_x \, \eta \, dA \qquad (28)$$

The incremental bending stress $\Delta\sigma_x$ is given by Eq. (26) and σ_x is obtained.

Liquid Sodium Effect: Very limited creep test data of 304 stainless steel submerged in liquid sodium have shown that the tensile creep rate of thin sheet in liquid sodium is much higher than that in air. Since the process tube is in contact with liquid sodium, this process tube is analyzed and checked for a life of 10×10^6 hours instead of its designed life of 200,000 hours this allows an increase of 50 times in the creep rate due to the presence of sodium.

Corrosion Effect: The wall thickness decreases with time of operation due to corrosion. It has been estimated that the wall thickness is reduced by 4 mils at 750% to 17 mills at 1190°F in 24 years of tube life. One quarter of this thickness reduction caused by corrosion is deducted for each quarter of the tube life.

3. RESULTS AND CONCLUSIONS

The deflection curves at different stages of tube life are plotted in Fig. 7. It is seen that the maximum deflection decreases from 0.825" at x = 125" at zero time to 0.712" at x = 150" at 100,000 hours. This is due to creep relaxation causing large curvature near the top. The internal pressure is larger at the lower end than near the top. Creep bowing tends to shift the point of maximum deflection forward the lower end. Beyond 100,000 hours, maximum deflection increases and the point of maximum deflection moves downward. At 10,000,000 hours, the tube deflection is not excessive. Assuming that liquid sodium increases the creep rate, not more than 50 times, this process tube is satisfactory in buckling for 200,000 hours. The change of tube length is less than 0.10 in for the whole life, so this has no significant effect on the initial tension of the bellow. The maximum longitudinal stress σ_x in the tube vs. time is shown in Fig. 8. The average of this stress over this life is close to 1000 p.s.i., which is much less than the rupture stress for 200,000 hours. Hence, this tube is considered to be satisfactory. This method has also been satisfactorily applied to study the effect of tube temperature, wall thickness, angle of inclination β, and internal pressure on the tube.

REFERENCES

[1] SHANLEY, F.R., "Applied Column Theory," Trans. Am. Soc. Civil Engrs., Vol. 115, p. 698, (1950).

[2] SHANLEY, F.R., Weight-Strength Analysis of Aircraft Structures, McGraw-Hill Book Co., p. 356, (1952).

[3] HIGGINS, T.P. Jr., "Effect of Creep on Column Deflection," Preprint No. 385, Inst. Aero. Science, (1952).

[4] LIBOVE, C., "Creep Buckling of Columns," Jour. Aero. Science, Vol. 19, pp. 459-467, (1952).

[5] HOFF, N.J., "A Survey of the Theories of Creep Buckling," Proc. 3rd U.S. Nat. Cong. Appl. Mech., (1958).

[6] LIN, T.H., "Creep Stresses and Deflections of Columns," Jour. Appl. Mech., Vol. 78, pp. 214-218, (1956).

[7] LIN, T.H., "Creep Deflections and Stresses of Beam-Columns," Jour. Appl. Mech Mech., Vol. 80, pp. 75-78, (1958).

[8] McVETTY, P.G., "Creep of Metals at Elevated Temperatures-The Hyperbolic Sine Relation Between Stress and Creep Rate," Trans. ASME, Vol. 65, p. 761, (1943).

[9] NADAI, A., The Influence of Time Upon Creep, The Hyperbolic Sine Law, S. Timoshenko Anniversary Volume, McMillan Co., p. 155, (1938).

[10] LIN, T.H., Theory of Inelastic Structures, John Wiley & Sons, p. 64, (1969).

[11] JOHNSON, A.E. and HENDERSON, J., "Complex Stress Creep Relaxation and Fracture of Metallic Alloys," Her Majesty' s Stationary Office, Edingburgh, England, (1962).

[12] HILL, R., The Mathematical Theory of Plasticity, The Clarendon Press, Oxford, England, p. (1950).

[13] SODERBERG, C.R., "The Interpretation of Creep Tests for Machine Design," Trans. A.S.M.E., Vol. 58, p. 733, (1936).

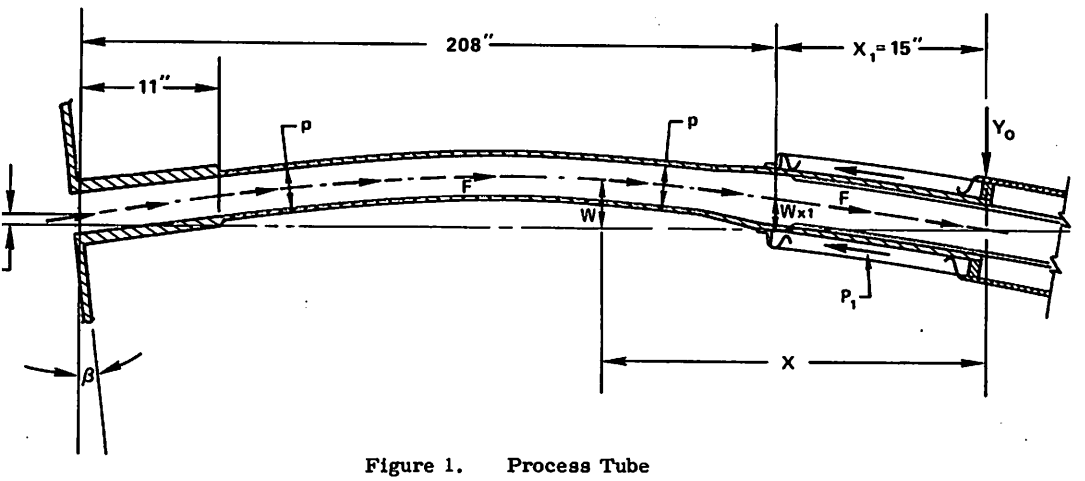

Figure 1. Process Tube

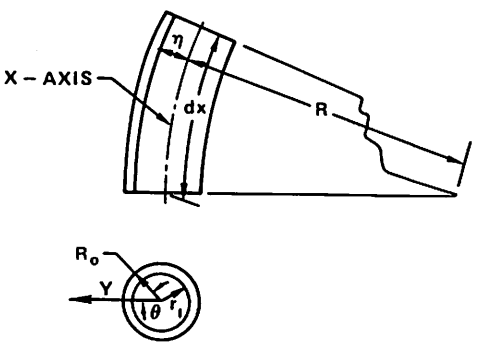

Figure 2. A Segment of the Tube in Bending

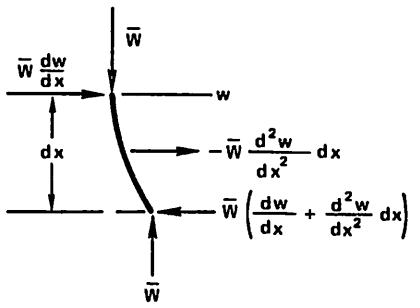

Figure 3. Deflected Fuel Elements

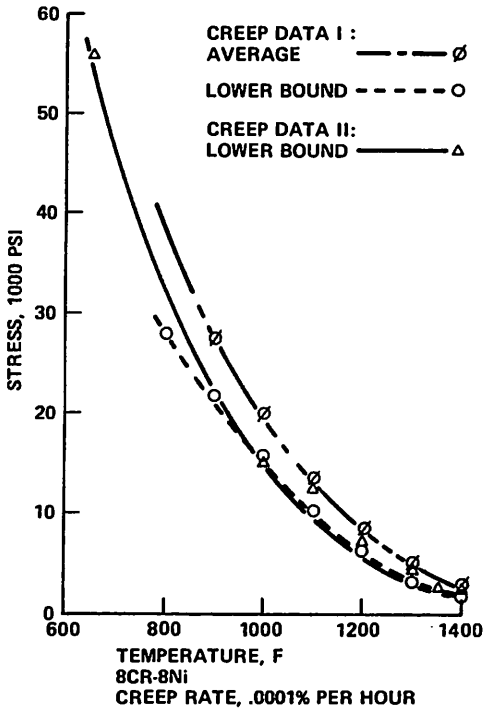

Figure 4. Creep Data of 304 Stainless Steel @ Creep Rate of .0001% per Hour

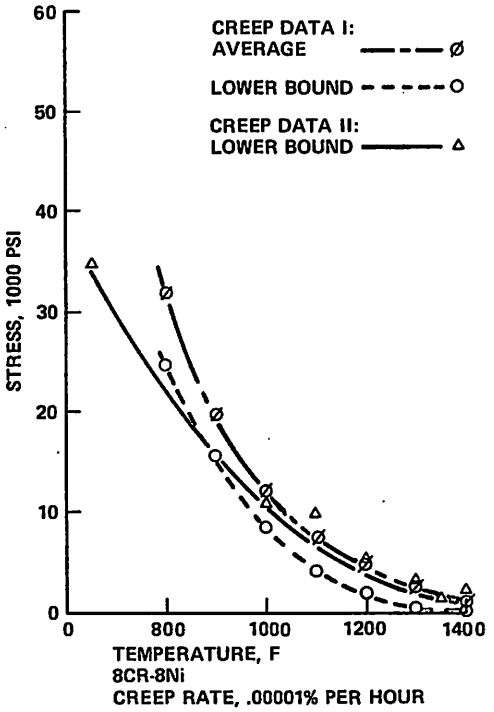

Figure 5. Creep Data of 304 Stainless Steel @ Creep Rate of .00001% per hour

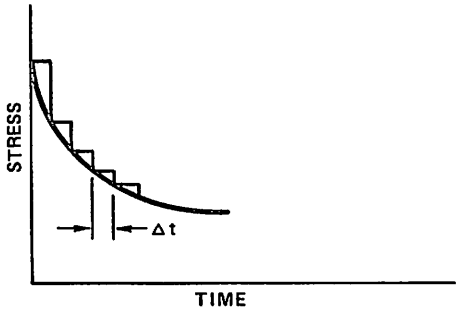

Figure 6. Approximation of the Smooth Stress-time Curve by Steps

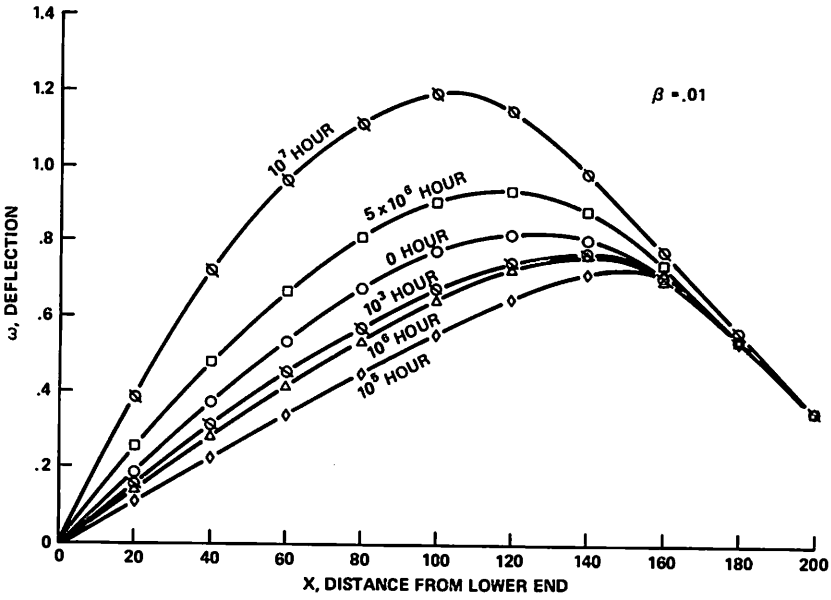

Figure 7. Deflection Curves of the Process Tube

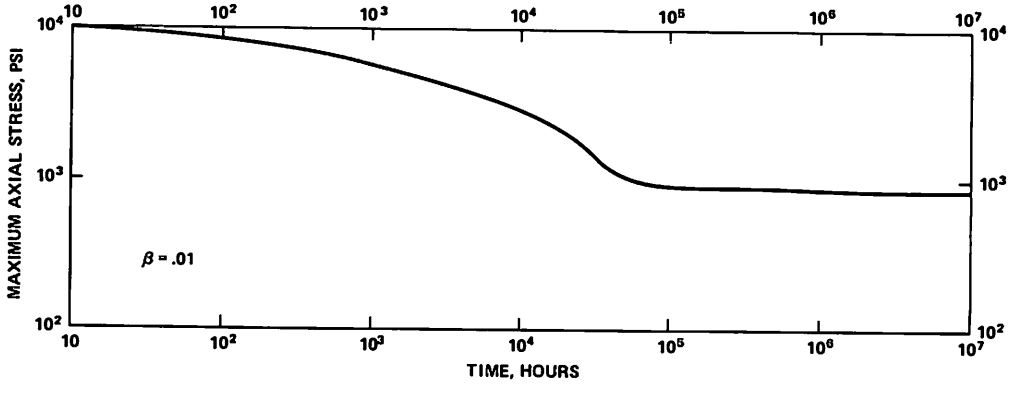

Figure 8. Maximum Longitudinal Stress vs Time Curve of the Process Tube

DISCUSSION

Q W. L. GREENSTREET, U. S. A.

1. How important was the unbalance in lateral pressure to the deflection in comparison to the other contributing factors ?

2. What was the criterion for buckling used, for example, was buckling defined when deflection rate (maximum) reached a certain value ?

A W. F. ANDERSON, U. S. A.

1. The area πa^2 times the net internal pressure $p_i - p_o$, where "a" is the internal radius, has the same effect as the compressive load on the column. This internal pressure varies from 15 psi at the top to 22 psi at the bottom and the internal radius is 2 inches. The total fuel element weight is 263 lbs. Hence the equivalent compressive load caused by the net internal pressure is quite significant.

2. In the present case, the maximum lateral deflection developed in the life of the process tube was used as the criterion for the tube design.